



## Molecular Docking, Synthesis and ADME Studies of New Pyrazoline Derivatives as Potential Anticancer Agents



CrossMark

Ammar K. Wabdan<sup>1,2\*</sup>, Monther F. Mahdi<sup>2</sup>, Ayad K. Khan

<sup>1</sup>Almuthana Health Directorate – Ministry of Health, Iraq.

<sup>2</sup>Department of Pharmaceutical Chemistry, College of Pharmacy, Mustansiriyah University, Baghdad, Iraq.

### Abstract

Cancer is a significant worldwide public health issue. The adverse effects of anticancer chemotherapies still compromise the quality of life of patients. To identify new potential targeted anticancer agents, a series of pyrazoline derivatives were synthesized and evaluated for anticancer effects on A549 (human lung adenocarcinoma cell line). In silico evaluation methods were done before synthesis through molecular docking via genetic optimization for ligand docking (GOLD) Suite software with EGFR tyrosine kinase and exhibited significant tyrosine kinase inhibition activities compared with Erlotinib as a reference drug due to their hydrogen bonding and short contact interaction with key amino acids and these results are compatible with the experimental findings. The new derivatives were synthesized by incorporating pyrazoline pharmacophore into nabumetone moiety as a starting molecule and the chalcone derivatives as intermediate products. The compounds structure were confirmed by <sup>1</sup>H-NMR, some physicochemical properties and infrared spectroscopy. An in vitro assay demonstrated that the final compounds (P1, P2, P3 and P4) exerted potent to moderate cytotoxic activity in the micromolar range with an IC<sub>50</sub> values (15.409 μM, 7.24 μM, 27.05 μM, 22.45 μM) respectively when compared with Erlotinib (IC<sub>50</sub> = 25.23 μM) while (P5&P6) show weak activity. Pharmacokinetic and physicochemical properties of the final compounds predicted by using ADME evaluations. The results showed all the synthesized compounds have high oral bioavailability and good GI absorption.

**Keywords:** Nabumetone ; Pyrazoline ; Docking studies ; ADME studies ; Cytotoxic assay.

### Introduction

Cancer is a complex disease characterized by development of abnormal cells that divide uncontrollably that are capable of dedifferentiation, invasion and metastasis through the lymphatic system or blood stream <sup>(1,2)</sup>.

Cancer is considered one of the most severe health problems and leading cause of mortality in the world<sup>(3,4)</sup>. In the past few years, apart from the usefulness of surgical operations and irradiation, chemotherapy still remains an important choice in treatment of cancer<sup>(5)</sup>. Resistance to chemotherapeutic agents<sup>(6)</sup>, lack of selectivity<sup>(7)</sup>, and serious adverse effects are the primary challenges in the treatment of cancer<sup>(8)</sup>. Therefore there is a need to discover a new and most safe anticancer agents with a broader spectrum of cytotoxicity to cancer cells<sup>(9)</sup>.

A potential solution is to explore innovative natural

pharmacophore to treat cancer<sup>(10)</sup>. Medicinal chemists have executed many research on pyrazoline derivatives due to their various therapeutic applications, range from central nervous system activity to antimicrobial applications<sup>(11,12)</sup>. Furthermore, a significant amount of research has shown that heterocycles based pyrazole show promising activity against cancer cell lines, including A549 human lung adenocarcinoma and liver cancer cell lines<sup>(13-15)</sup>.

This pharmacologically-interesting heterocyclic system have been synthesized from the reaction of α,β-unsaturated ketones (chalcone) (1) that have a wide range of pharmacological activities, including antioxidant, anti-tumor, antibacterial, antihistaminic, antifungal, anticancer, antiobesity, anti-inflammatory, anti-spasmodic, anti-malarial, anti-protozoal and cytotoxic properties<sup>(16)</sup> with benzohydrazide derivatives.

Pyrazoline (2) showed good inhibitory activity

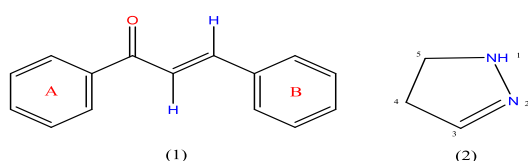
\*Corresponding author e-mail: [ayad@uomustansiriyah.edu.iq](mailto:ayad@uomustansiriyah.edu.iq); (Ayad Kareem Khan).

Receive Date: 21 February 2021, Revise Date: 2 April 2021, Accept Date: 18 April 2021

DOI: 10.21608/EJCHEM.2021.64042.3377

©2021 National Information and Documentation Center (NIDOC)

against the proliferation of A549 and other cancer cells<sup>(15)</sup>. Structure-activity. relationship (SAR) studies exhibit that the activity of pyrazoline derivatives is dependent on the presence of the nitrogen heterocyclic moiety<sup>(17)</sup>, a structural subunit which is considered to have a number of pharmacological properties and widespread biological medical activities<sup>(18)</sup>. Furthermore, most pyrazoline derivatives are chiral molecules, provided a greater degree of variability in substitutions and conformation, leading to better biological activity<sup>(19)</sup>. Therefore, a series of new pyrazoline derivatives has been synthesized from nabumetone as starting molecule and evaluated for their anticancer activity after the good activity obtained from docking studies.



## Experimental

### Materials and Methods:

All reagents and solvents were received from the commercial suppliers (SOLVOCHEM, England, Pancreac, Spain, Sigma-Aldrich, Germany and BDH, England). Nabumetone and benzohydrazide derivatives were supplied by the Shanghai Renyoung Company, China. Cancer cell lines A549 received from ATCC, USA. Melting points were determined by Stuart Electric melting point apparatus (England). The identification of compounds was achieved by using IR spectrum were recorded on Shimadzu FT-IR infrared spectrometer, performed by using KBr disks. <sup>1</sup>H-NMR determined by Varian, Agilent 500 MHz (USA).

### Chemical synthesis:

The synthesis of intermediates and final compounds was done by using the procedures illustrated in (Scheme 1).

### General procedure for chalcone derivatives synthesis (C1&C2):

Sodium hydroxide (0.088 g, 2.2 mmol) dissolved in 7.5 mL of absolute methanol: D.W (2:1) with stirring for (15 min.). (0.5 g, 2.2 mmol) of nabumetone dissolved in 15 mL of diethyl ether: methanol (2:1) solvent system with stirring for (10 min.) until the compound will completely dissolve, then benzaldehydes derivatives (a-b) (2.2 mmol) added to the mixture of nabumetone. The mixture was exposed to an ultrasonic generator in a water bath at (35 °C) for (25 min.) which was then allow for

stirring for 24 hours. The mixture then filtered and washed with cold water until the mixture became neutral to the litmus paper. The filtered precipitate left to dry and then washed with ether.<sup>(20)</sup>

### General procedure for pyrazoline derivatives synthesis (P1-P6):

A mixture of chalcone derivatives (C1 and C2) (1.0 mmol) and benzohydrazide derivatives

(1.0 mmol) in 20 mL of absolute ethanol was refluxed, after (15 min.) add two drops of glacial acetic acid, and the contents allowed getting reflux for (24 hrs.). (20 mL) Cold water added to the mixture to precipitate out the product. The product then filtered and washed twice with cold water, and finally dried.<sup>(21)</sup>

**1-(4-Chlorophenyl)-5-(6-methoxynaphthalen-2-yl)pent-1-en-3-one (C1):** White powder (95% yield); mp 128–130°C; IR (KBr)  $\nu$  (cm<sup>-1</sup>): 1683.91 (C=O), 1606.06 (C=C aromatic), 1265.35 (C–O–CH<sub>3</sub>) ; <sup>1</sup>H-NMR (DMSO-d<sub>6</sub>, 500 MHz):  $\delta$  2.96 (t, 2H, CH<sub>2</sub>–CH<sub>2</sub>),  $\delta$  3.35 (t, 2H, CH<sub>2</sub>–CH<sub>2</sub>),  $\delta$  3.84 (s, 3H, O–CH<sub>3</sub>),  $\delta$  6.57 (d, 1H, CH=CH),  $\delta$  7.50 (d, 1H, CH=CH),  $\delta$  7.12–7.81 (m, 10H, Ar H).

**1-(4-(Dimethylamino)phenyl)-5-(6-methoxynaphthalen-2-yl)pent-1-en-3-one (C2):** Yellow buff powder (71% yield); mp 134–136°C; IR (KBr)  $\nu$  (cm<sup>-1</sup>): 1633.76 (C=O), 1521.89 (C=C aromatic), 1261.46 (C–O–CH<sub>3</sub>), 1165.04 (N–CH<sub>3</sub>) ; <sup>1</sup>H-NMR (DMSO-d<sub>6</sub>, 500 MHz):  $\delta$  2.95 (s, 6H, N(CH<sub>3</sub>)<sub>2</sub>), 3.01 (t, 2H, CH<sub>2</sub>–CH<sub>2</sub>),  $\delta$  3.33 (t, 2H, CH<sub>2</sub>–CH<sub>2</sub>),  $\delta$  3.82 (s, 3H, O–CH<sub>3</sub>),  $\delta$  6.58 (d, 1H, CH=CH),  $\delta$  7.08 (d, 1H, CH=CH),  $\delta$  7.12–7.75 (m, 10H, Ar H).

**(5-(4-chlorophenyl)-3-(2-(6-methoxynaphthalen-2-yl)ethyl)-4,5-dihydro-1H-pyrazol-1-yl) (phenyl)methanone (P1):** Yellowish white crystals (63% yield); mp 173–175°C; IR (KBr)  $\nu$  (cm<sup>-1</sup>): 1668.48 (C=O), 1606.49 (C=N of diazole), 1516.1 (C=C aromatic), 1240.27 (C–O–CH<sub>3</sub>), 1168.9 (C–N of diazole); <sup>1</sup>H-NMR (DMSO-d<sub>6</sub>, 500 MHz):  $\delta$  2.46 (t, 2H, CH<sub>2</sub> CH<sub>2</sub>),  $\delta$  2.85 (t, 2H, CH<sub>2</sub> CH<sub>2</sub>),  $\delta$  3.38 (d, 2H, diazole CH<sub>2</sub>),  $\delta$  3.85 (s, 3H, O–CH<sub>3</sub>),  $\delta$  5.35 (t, 1H, diazole CH),  $\delta$  6.55–7.82 (m, 14H, Ar H).

**(5-(4-chlorophenyl)-3-(2-(6-methoxynaphthalen-2-yl)ethyl)-4,5-dihydro-1H-pyrazol-1-yl)(4-hydroxyphenyl)methanone (P2):** Yellowish white powder (60% yield); mp 219–121°C; IR (KBr)  $\nu$  (cm<sup>-1</sup>): 3263.3 (broad O–H), 1647.26 (C=O), 1606.76 (C=N of diazole), 1491.02 (C=C aromatic), 1226.77 (C–O–CH<sub>3</sub>), 1174.69 (C–N of diazole) ; <sup>1</sup>H-NMR (DMSO-d<sub>6</sub>, 500 MHz):  $\delta$  2.42 (t, 2H, CH<sub>2</sub>–CH<sub>2</sub>),  $\delta$

2.77 (t, 2H, CH<sub>2</sub>-CH<sub>2</sub>),  $\delta$  3.06 (d, 2H, diazole CH<sub>2</sub>),  $\delta$  3.82 (s, 3H, O-CH<sub>3</sub>),  $\delta$  5.38 (t, 1H, diazole CH),  $\delta$  6.48–7.78 (m, 14H, Ar H),  $\delta$  9.91 (s, 1H, OH).

**(4-aminophenyl)(5-(4-chlorophenyl)-3-(2-(6-methoxynaphthalen-2-yl)ethyl)-4,5-dihydro-1H-pyrazol-1-yl)methanone (P3):** off-white powder (68% yield); mp 138–140°C; IR (KBr)  $\nu$  (cm<sup>-1</sup>): 3346.6 (N-H), 1654.98 (C=O), 1602.9 (C=N of diazole), 1506.2 (C=C aromatic), 1246.06 (C-O-CH<sub>3</sub>), 1180.47 (C-N of diazole); <sup>1</sup>H-NMR (DMSO-d<sub>6</sub>, 500 MHz):  $\delta$  2.41 (t, 2H, CH<sub>2</sub>-CH<sub>2</sub>),  $\delta$  2.93 (t, 2H, CH<sub>2</sub>-CH<sub>2</sub>),  $\delta$  3.14 (d, 2H, diazole CH<sub>2</sub>),  $\delta$  3.81 (s, 3H, O-CH<sub>3</sub>),  $\delta$  4.36 (s, 2H, NH<sub>2</sub>),  $\delta$  5.72 (t, 1H, diazole CH),  $\delta$  6.48–7.78 (m, 14H, Ar H).

**(5-(4-(dimethylamino)phenyl)-3-(2-(6-methoxynaphthalen-2-yl)ethyl)-4,5-dihydro-1H-pyrazol-1-yl)(4-fluorophenyl)methanone (P4):** Orange powder (71% yield); mp 148–150°C; IR (KBr)  $\nu$  (cm<sup>-1</sup>): 1660.77 (C=O), 1631.83 (C=N of diazole), 1520.82 (C=C aromatic), 1228.7 (C-O-CH<sub>3</sub>), 1124.54 (C-N of diazole), 1165.04 (N-CH<sub>3</sub>); <sup>1</sup>H-NMR (DMSO-d<sub>6</sub>, 500 MHz):  $\delta$  2.46 (t, 2H, CH<sub>2</sub>-CH<sub>2</sub>),  $\delta$  2.94 (s, 6H, N(CH<sub>3</sub>)<sub>2</sub>),  $\delta$  3 (t, 2H, CH<sub>2</sub>-CH<sub>2</sub>),  $\delta$  3.03 (d, 2H, diazole CH<sub>2</sub>),  $\delta$  3.85 (s, 3H, O-CH<sub>3</sub>),  $\delta$  5.83 (t, 1H, diazole CH),  $\delta$  6.60–7.96 (m, 14H, Ar H).

**(4-aminophenyl)(5-(4-(dimethylamino)phenyl)-3-(2-(6-methoxynaphthalen-2-yl)ethyl)-4,5-dihydro-1H-pyrazol-1-yl)methanone (P5):** Yellow powder (50% yield); mp 168–170°C; IR (KBr)  $\nu$  (cm<sup>-1</sup>): 3377.47 (N-H), 1639.577 (C=O), 1604.83 (C=N of diazole), 1519.96 (C=C aromatic), 1271.13 (C-O-CH<sub>3</sub>), 1124.54 (C-N of diazole), 1178.55 (N-CH<sub>3</sub>); <sup>1</sup>H-NMR (DMSO-d<sub>6</sub>, 500 MHz):  $\delta$  2.41 (t, 2H, CH<sub>2</sub> CH<sub>2</sub>),  $\delta$  2.94 (s, 6H, N(CH<sub>3</sub>)<sub>2</sub>),  $\delta$  3.05 (t, 2H, CH<sub>2</sub> CH<sub>2</sub>),  $\delta$  3.3 (d, 2H, diazole CH<sub>2</sub>),  $\delta$  3.89 (s, 3H, O-CH<sub>3</sub>),  $\delta$  4.35 (s, 2H, NH<sub>2</sub>),  $\delta$  5.75 (t, 1H, diazole CH),  $\delta$  6.42–7.78 (m, 14H, Ar H).

**(5-(4-chlorophenyl)-3-(2-(6-methoxynaphthalen-2-yl)ethyl)-4,5-dihydro-1H-pyrazol-1-yl)(4-fluorophenyl)methanone (P6):** Yellow powder (91% yield); mp 174–176°C; IR (KBr)  $\nu$  (cm<sup>-1</sup>): 1668.48 (C=O), 1649.19 (C=N of diazole), 1520.82 (C=C aromatic), 1236.41 (C-O-CH<sub>3</sub>), 1122.61 (C-N of diazole); <sup>1</sup>H-NMR (DMSO-d<sub>6</sub>, 500 MHz):  $\delta$  2.46 (t, 2H, CH<sub>2</sub> CH<sub>2</sub>),  $\delta$  2.88 (t, 2H, CH<sub>2</sub> CH<sub>2</sub>),  $\delta$  3.17 (d, 2H, diazole CH<sub>2</sub>),  $\delta$  3.85 (s, 3H, O-CH<sub>3</sub>),  $\delta$  6.92 (t, 1H, diazole CH),  $\delta$  6.95–7.97 (m, 14H, Ar H).

#### Computational methods: ADME procedures

Physicochemical and pharmacokinetic properties of all ligands (P1-P6) were determined by using SwissADME server. The chemical structure of designed compounds drawn by using Chem. Sketch (v. 12) and then converted by Swiss ADME tool to SMILE name.<sup>(22)</sup>

#### Docking Studies

The molecular docking studies are a beneficial tool for the evolution of new compounds with prediction of ligand-receptor interaction, and the biological activity of designed compounds. CCDC GOLD Suite (v. 5.7.1) include Hermes visualizer software (v. 1.10.1), used for visualization of receptors, ligands, type of interaction (H-bond, short contact ...etc.), active site, bond length calculation<sup>(23)</sup>.

#### Ligand and receptor preparation

The chemical structure of our ligands was drawn primarily using ChemDraw professional software (v.16.0). CheBio3D (v. 17.1) was used for energy minimization of our synthesized ligands. The crystal structure of the enzyme EGFR tyrosine kinase [PDB ID: 4HJO]<sup>(24)</sup> was downloaded from the Protein Data Bank (PDB). The crystal structure of the downloaded protein was prepared by adding hydrogen atoms and by removing water molecules not involved in the active site to get a correct tautomeric states and ionization of amino acid residues.

#### Molecular docking protocol

HERMES –Structure visualization software of GOLD Suite was used for setup of the receptors for the docking process. The reference ligand of the protein was used to determine the radius (10 Å) of the active site. ChemScore kinase has been used as a configuration template. ChemPiecewise linear potential (CHEMPLP) was used for the scoring function. The values of all parameters used during the process of docking were kept the default, and all solutions are scored according to CHEMPLP fitness function. The docking results such as the docked pose, binding mode, and binding free energy was used to assess the ligands interaction with the protein residues of the tyrosine kinase enzyme.

#### Cytotoxic assay

The methodology used to investigate the anticancer activity of (P1-P6) on viability of **Lung Cancer Cell Line (A549)** by MTT assay<sup>(25)</sup> was carried out at the College of Pharmacy/ Mustansiriyah University, Iraq.

### Cell Culture and Maintenance

Lung Cancer Cell Line (A549) was originally obtained ATCC. The storage of it was in the Cell Bank of the Tissue Culture Research Center at Mustansiriyah University / College of pharmacy. A549 cells were maintained in Roswell Park Memorial Institute-1640 (RPMI-1640) medium supplemented with 10% fetal bovine serum FBS and 1% L-Glutamine as well as to 1% Penicillin-Streptomycin-Amphotericin B 100X as antiseptic<sup>(26)</sup>.

### Cell Viability by MTT Assay

The MTT assay was used for analysis the effects of (P1-P6) on the viability of lung cancer cells. A 100  $\mu$ l from A549 cell's suspensions were dispensed into 96- well flat-bottom tissue culture plates at concentrations of ( $5 \times 10^3$  cells/well) and incubated for 24 h under standard conditions, ( $4 \times 10^3$  cells per well) incubated for 48 h and ( $3 \times 10^3$  cells per well) incubated for 72 h. After complete 24 h, the cells were treated with (0.9, 1.8, 3.25, 7.5, 15 and 30  $\mu$ g/mL). Following a recovery period 24 h, 48 h and 72 h, the cell culture medium was removed and cultures were incubated with medium was contained 30  $\mu$ L solution of MTT (3 $\mu$ g/mL MTT in PBS) (3-\4,5-Dimethylthiazol-2-yl)-2,5-Diphenyltetrazolium Bromide) at 37° C for 4 hr. After the end of 4 hr this medium was removed by smooth inversion and tapping onto paper. The Control wells received only 100  $\mu$ L from growth media. Then 100  $\mu$ L of dimethyl sulfoxide (DMSO) was added to each well and kept the plates were at room temperature in the dark conditions for about 15-20 min. The measuring of absorbance of each well was by using multiscan reader instrument at a wavelength (540 nm) and the correction for background absorbance using (650 nm) wavelength<sup>(27)</sup>.

The assay was performed in a triplicate and the percent of inhibition rate (percentage of cytotoxicity) was calculated by: [Inhibition Rate percentage= (A-B/A) \* 100].

Were A and B is the optical density for Erlotinib (control) and optical density of test respectively.

### The Half Maximal Inhibitory Concentration (IC<sub>50</sub>) Value Determination:

The determination of IC<sub>50</sub> of the drug can be done by assembling a dose-response curve and analyzing the effect of different concentrations of the antagonist on exchanging agonist activity. IC<sub>50</sub> values can be measured for a given antagonist through determining the concentration that required inhibiting half of the maximum biological response of the agonist. IC<sub>50</sub> values are highly dependent on

the requirements under which they are measured. Generally, the large agonist activity will be lowered when the higher concentration of inhibitor used. IC<sub>50</sub> value rises as agonist concentration increases. Besides, IC<sub>50</sub> value influenced depending on the type of inhibition of other factors. According to the in vitro MTT assay, the IC<sub>50</sub> represents the concentration of the tested (P1-P6) compounds that is required for 50% inhibition of the cell viability. Based on the obtained data using the in vitro MTT assay, the IC<sub>50</sub> values for (P1-P6) compounds at 72 h after the cells exposure to these compounds. To determine the IC<sub>50</sub> values, the concentration range used was 0.9 - 30  $\mu$ g/ml<sup>(28)</sup>.

### Statistical analysis

Statistical analyses of IC<sub>50</sub> and MTT assay data of tested compounds [P1-P6] on A549 cells were done by using Graphpad Prism utilizing the nonlinear curve fitting software. One-way ANOVA with Tukey test was used to Compare all groups within the same plate of MTT was evaluated by (prism and software). Values of  $p > 0.05$  were considered statistically significant.

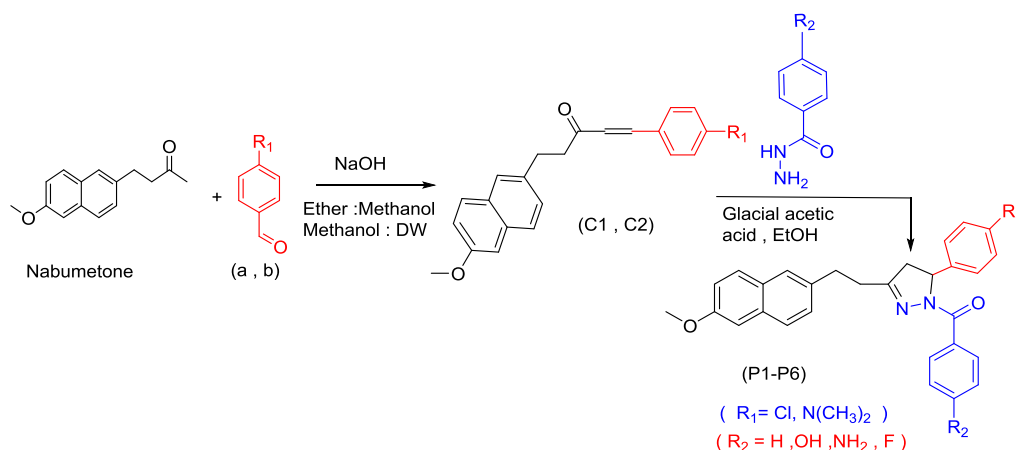
## RESULTS AND DISCUSSION

### ADME results interpretation:

The ADME properties results of the final synthesized compounds were studied by Swiss ADME server<sup>(22)</sup> to reveal the safest and potential drug candidate(s), to exclude the compounds that may be fail in the next stages of the drug development because of the inappropriate ADME properties<sup>(29)</sup>.

We assessed all synthesized compounds pharmacokinetic properties (absorption, distribution, metabolism, excretion). Topological polar surface area (TPSA) was estimated, since it is a very important property to determine the degree of drug bioavailability<sup>(30)</sup>. Thus, passively absorbed molecules with a TPSA >140 Å<sup>2</sup> are thought to have low oral bioavailability. The results of our all synthesized compounds showed that TPSA below 140, which is in the range (26.3 – 71.16) and the bioavailability for all ligands was 0.55 which means that all ligands reach the systemic circulation, as shown in the **Table (1)**

The GI absorption score refer to the amount of extent of absorption of a molecule from the intestine after oral administration. The absorption could be excellent if the result were high. In our study, the GI absorption of all synthesized ligands was high expecting them to be well absorbed from the intestine.



**Scheme (1): Synthesis of intermediates and target compounds.**

### Interpretation of docking results:

GOLD (Genetic Optimisation for Ligand Docking) is a genetic algorithm for docking flexible ligands into protein binding sites<sup>(31)</sup>. GOLD Suite has shown perfect performance for pose prediction and excellent results for virtual screening.<sup>(32)</sup>

GOLD is a part of CSD-Discovery, which include other softwares such as Hermes, CSD python, Mercury, Isostar, ConQuest, Mogul and others. Hermes gives the GOLD's graphical user interface, it is designed to aid the preparation of input information of GOLD docking, visualization of dock results and calculation of descriptors.

Successful docking was done using GOLD Suite software for all newly synthesized compounds (**P1-P6**).

Energy minimization for ligands which means that a minimal amount of energy has been obtained is required to correct distorted geometries by changing the geometry of the molecule structure in order to release internal constraints.

The docking results to predict the selectivity and binding energies of the ligands for the protein (EGFR) through studying the contact interactions among the active binding sites of the protein, and designed compounds. The EGFR inhibitory activity of compounds (P1-P6), and Erlotinib, were ranked based on their PLP fitness. The PLP fitness of the docked compounds on EGFR tyrosine kinase was found in the range of **81.11 to 90.52 (Table 2)**. There is an excellent agreement between our docked results and the experimental results (*In vitro* study).

**Table (1) ADME results of intermediates and target compounds.**

Comp.	Molecular Refractivity	Topological Polar Surface Area (TPSA)	GI Absorption	BBB permeability	Bioavailability
C1	104.65	26.30	High	YES	0.55
C2	113.85	29.54	High	YES	0.55
P1	145.55	41.90	High	No	0.55
P2	147.58	62.13	High	No	0.55
P3	149.69	67.92	High	No	0.55
P4	154.71	45.14	High	No	0.55
P5	159.16	71.16	High	No	0.55
P6	145.51	138.58	High	No	0.56

**Table (2) The binding energies for target compounds (P1-P6) and standard TKIs Erlotinib docked with EGFR**

Compound	EGFR Binding Energy (PLP Fitness)	Amino Acids Included in H-bonding	Amino Acids Included in Short Contact Interactions
P1	90.52	CYS773	LEU694 ,LEU764(4)*, LEU753, LEU834, PHE832 ,GLY695 ,CYS773(3)* , GLY772(2)*ALA719 , MET769(2)* , and THR766
P2	89.28	MET769(2) *	CYS751 ,LEU753(2)* ,MET742(3)* , VAL702 ,ASP831 ,LEU764 ,ARG817 , MET769(3)* THR830(2)* and PHE832(3)*
P3	82.3	THR766 LYS704	PRO770, LYS704, MET769(2)* ,ARG817 , ASP831 and THR766(3)*
P4	87.36	GLY695	GLY695 ,LEU694 ,ASP831 ,LEU753 , MET742 ,PHE832 and VAL702
P5	86.5	ASP831 THR766 LYS704	ASP831 ,ASN818 ,ARG817 ,THR766(2)* , PRO770 ,MET769(2)* and LYS704
P6	81.11	LYS704 THR766	MET769 ,THR766 ,ASP831 ,ALA719 and GLU767
Erlotinib	85.8	CYS773 MET769 LYS704	LEU694(3)* ,PRO770 ,MET769(4)* ,PHE771, LYS704 ,CYC773(3)* ,ASP831 ,GLY772(2), THR766(2)* ,GLN767 and LEU768(2)*

\*Number in brackets refer to no. of H-bonds.

GOLD software also gives the distance of hydrogen bonding between our ligands and a target protein as well as all bonds length was  $\leq 3\text{\AA}$  (33). Docking analysis indicated that ARG817, THR830, THR766, MET769, LEU694, LEU764, LEU834, GLU767, GLY695, CYS751, CYS773, ALA719, LEU753, MET742, VAL702, ASP831, PHE832, PRO770 and LYS704 amino acid residues of EGFR active site listed in (Table 2) interact through hydrogen bonding and short contacts with our final ligands library, and show promising activity with EGFR tyrosine kinase.

However, compounds [P1 and P2] show the highest PLP fitness value (90.52, 89.28) respectively, and H-bonding with amino acids as represented in Table (2).

Except P6 all other ligands exhibit higher binding energies than the standard drug Erlotinib that give PLP fitness value (85.8) and it is N-1 atom form H-bond with MET769, (O-CH<sub>3</sub>) group with LYS704 and the second (O-CH<sub>3</sub>) atom form H-bond through H<sub>2</sub>O Bridge with CYS773 in addition to short contact interactions as shown in Figure (1). As illustrated in Figure (2) compound P1 forms H-bond via C=O with CYS773 along with other short contacts that reinforce the binding and give PLP value (90,52). Compound P2 that give PLP fitness value (89.28) form two H-bond through O-H group with the MET769 along with short contact as shown in Figure (3). The H-bond and short contact interaction of the remain compounds listed in Table (2).

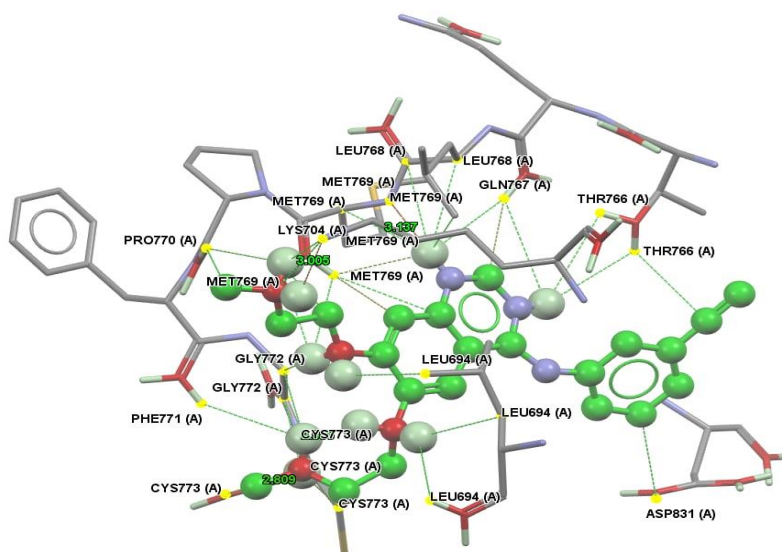


Figure (1) H-bond and short contact interaction profile for the standard drug Erlotinib binding with EGFR receptor (PDB code: 4HJO). The interaction between Erlotinib and amino acid residues by H-bond [MET769, LYS704, and CYS773], [Erlotinib: ball and stick style, while amino acids in capped sticks].

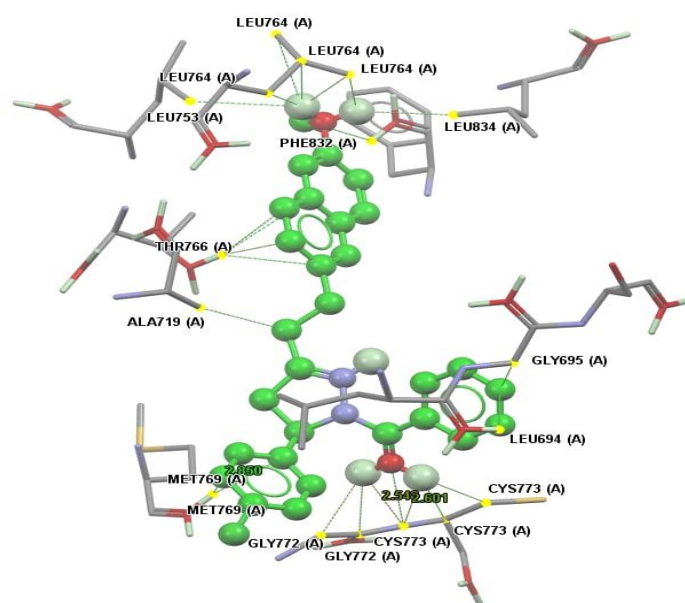
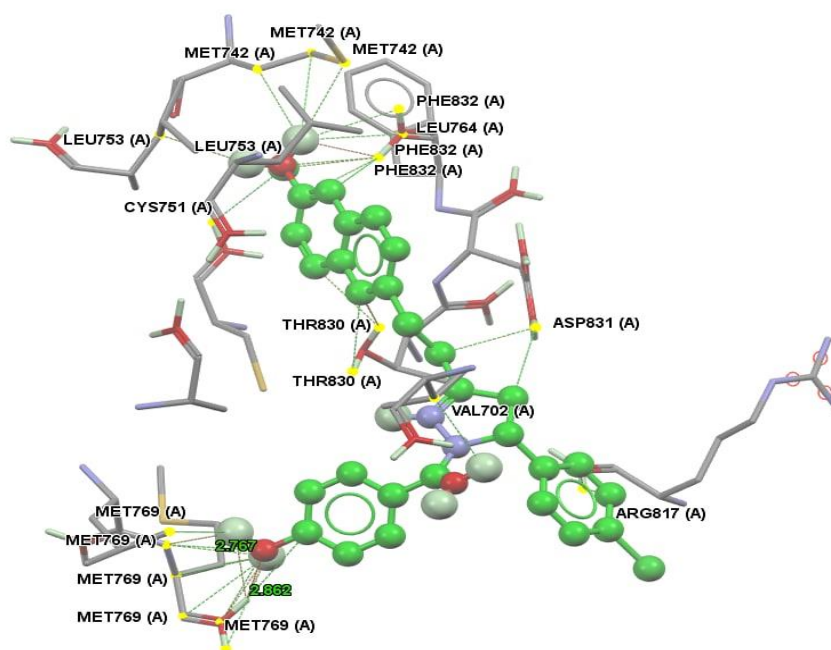


Figure (2) H-bond and short contact interaction profile for compound (P1) binding with EGFR receptor (PDB code: 4HJO). The interaction between compound (P1) and amino acid residues by H-bond [CYS773]. [P1: ball and stick style, while amino acids in capped sticks].



**Figure (3) H-bond and short contact interaction profile for compound (P2) binding with EGFR receptor (PDB code: 4HJO). The interaction between compound (P2) and amino acid residues by H-bond [MET769]. [P2: ball and stick style, while amino acids in capped sticks]**

### Results of cytotoxicity studies

The cytotoxic performed results of synthesized compounds [P1, P2, P3, P4, P5 and P6] showed promising anticancer activity. The best and more potent cytotoxic effect was for compound [P2] with an  $IC_{50}$  value of 7.24  $\mu$ M, considered as approximately threefold more active than Erlotinib with an  $IC_{50}$  value of 25.23  $\mu$ M and this means lower concentration from compound [P2] needed to inhibit cancerous A549 cell growth in comparison to Erlotinib<sup>(34)</sup>. Meanwhile, compounds [P1 and P4] exhibit significantly higher  $IC_{50}$  values (15.409, and 22.45)  $\mu$ M, respectively than the standard. While, Compound [P3] shows lower  $IC_{50}$  value of 27.05  $\mu$ M than the standard. Lastly, compound P5&P6 exert only a weak cytotoxic effect with  $IC_{50}$  more than 40  $\mu$ M. **Table (3)** summarized  $IC_{50}$  values for A549 cell line when treated for 72hr with compounds [P1, P2, P3, P4, P5 and P6] with a concentration (30  $\mu$ M) by using MTT assay. Figure (4) represent dose response curves of  $IC_{50}$  values.

The results also revealed that the percent of cell death is time-dependent increased with time from 24hr. to 72hr<sup>(35)</sup>. As shown in **Figure (5)** all the tested compounds show considerable variation in responsiveness to cell death compared to standard.

P2 compound exhibit cell death percentage (83.04%) higher than Erlotinib (82.40%) on the other hand compound (P3) was very close and slightly lower than Erlotinib with 81.21% of cell death. while compounds (P1 and P4) demonstrate high percentage of cell death but lower than Erlotinib. Further, compounds (P5 and P6) show the lowest percentage ranges from (35.51%-30.66%).

### Conclusion:

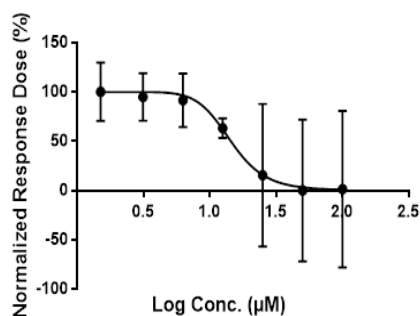
The chemical synthesis of a new pyrazoline derivatives compounds has been effectively achieved. Identification and characterization of the synthesized compounds have been verified by physical properties assurance (melting point and description), FT-IR and <sup>1</sup>HNMR spectra.

The anti-cancer evaluation of synthesized compounds against the A549 (lung) cancer cell line indicates these newly compounds exerts potent to moderate cytotoxic activity except for P5 and P6 showed weak activity. ADME studies showed that all designed compounds highly absorbed from The GIT. Docking studies showed a perfect compatibility with *in vitro* study.

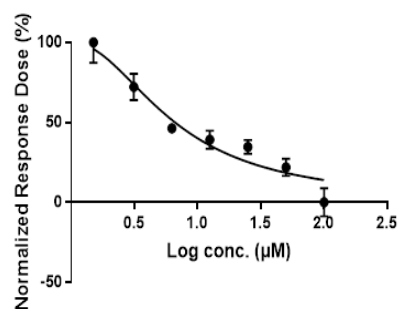
**Table (3) Cytotoxicity of the tested compounds (P1-P6) and Erlotinib as standard against A549 (lung cancer cell line**

Comp.	IC <sub>50</sub> (μM)
P1	15.409
P2	7.24
P3	27.05
P4	22.45
P5	>40
P6	>40
Erlotinib	25.23

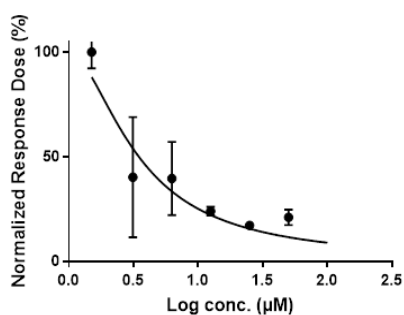
**P1** , IC<sub>50</sub>=15.409μM \ R<sup>2</sup>=0.99988



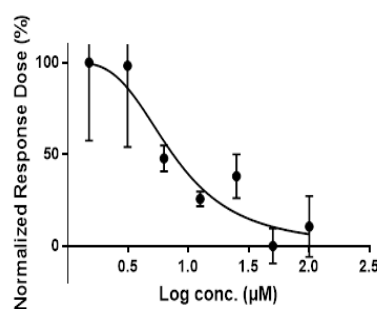
**P2** , IC<sub>50</sub>=7.24μM \ R<sup>2</sup>=0.99988

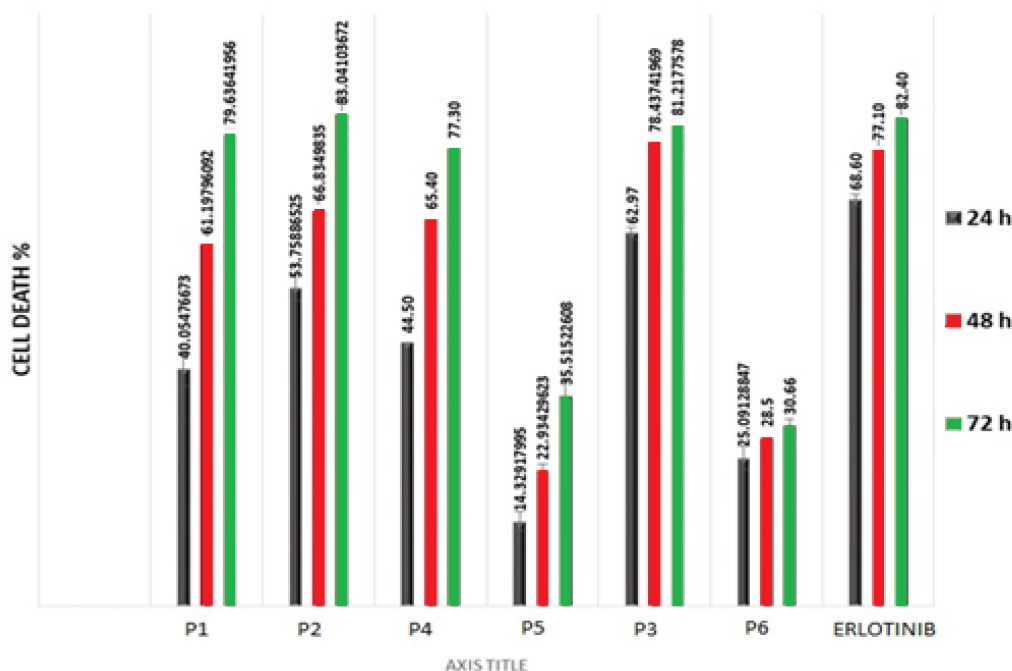


**P3** , IC<sub>50</sub>=27.05μM \ R<sup>2</sup>=0.9988



**P4** , IC<sub>50</sub>=22.45μM \ R<sup>2</sup>=0.99988

**Figure (4) Dose-response curves of IC<sub>50</sub> for A549 for compounds (P1-P4), treated for 72hr.**



Figure(5):A549 Cell Lines Death Percentage of P1, P2, P3, P4, P5 and P6 as compared with Erlotinib.

#### References :

- Henderson, H.P.R.J.R.R.J.F.G., Rang & Dale's pharmacology. 2016: Elsevier/Churchill Livingstone.
- Ghorab, M.M., M.G. El-Gazzar, and M.S. Alsaïd, Synthesis and anti-breast cancer evaluation of novel N-(guanidiny) benzenesulfonamides. International journal of molecular sciences, 2014. 15(4): p. 5582-5595.
- Seffrin, J.R., et al., It is time to include cancer and other noncommunicable diseases in the millennium development goals. 2009, Wiley Subscription Services, Inc., A Wiley Company Hoboken.
- Nepali, K., et al., Rational approaches, design strategies, structure activity relationship and mechanistic insights for anticancer hybrids. European journal of medicinal chemistry, 2014. 77: p. 422-487.
- Ramaswamy, B., et al., Phase II trial of pyrazoloacridine (NSC# 366140) in patients with metastatic breast cancer. Investigational new drugs, 2011. 29(2): p. 347-351.
- Nussbaumer, S., et al., Analysis of anticancer drugs: a review. Talanta, 2011. 85(5): p. 2265-2289.
- Kerbel, R., Molecular and physiologic mechanisms of drug resistance in cancer: an overview. Cancer and Metastasis Reviews, 2001. 20(1): p. 1
- Medina, P.P. and F.J. Slack, microRNAs and cancer: an overview. Cell cycle, 2008. 7(16): p. 2485-2492.
- Jin, C., et al., Synthesis and antitumor activity of ureas containing pyrimidinyl group. European journal of medicinal chemistry, 2011. 46(1): p. 429-432.
- Shaaban, M.R., A.S. Mayhoub, and A.M. Farag, Recent advances in the therapeutic applications of pyrazolines. Expert opinion on therapeutic patents, 2012. 22(3): p. 253-291.
- Kumar, S., et al., Biological activities of pyrazoline derivatives-A recent development. Recent patents on anti-infective drug discovery, 2009. 4(3): p. 154-163.
- Marella, A., et al., Pyrazolines: a biological review. Mini reviews in medicinal chemistry, 2013. 13(6): p. 921-931.
- Fahmy, H.H., et al., Biological validation of novel polysubstituted pyrazole candidates with in vitro anticancer activities. Molecules, 2016. 21(3): p. 271.
- Nitulescu, G.M., C. Draghici, and A.V. Missir, Synthesis of new pyrazole derivatives and their anticancer evaluation. European journal of medicinal chemistry, 2010. 45(11): p. 4914-4919.
- Strocchi, E., et al., Design, synthesis and biological evaluation of pyrazole derivatives as potential multi-kinase inhibitors in hepatocellular

- carcinoma. *European journal of medicinal chemistry*, 2012. 48: p. 391-401.
16. Yousif, O.A., M.F. Mahdi, and A.M. Raauf, Design, synthesis, preliminary pharmacological evaluation, molecular docking and ADME studies of some new pyrazoline, isoxazoline and pyrimidine derivatives bearing nabumetone moiety targeting cyclooxygenase enzyme. *Journal of Contemporary Medical Sciences*, 2019. 5(1).
  17. Kucukoglu, K., et al., Synthesis, cytotoxicity and carbonic anhydrase inhibitory activities of new pyrazolines. *Journal of enzyme inhibition and medicinal chemistry*, 2016. 31(sup4): p. 20-24.
  18. Lobo, P.L., et al., Synthesis, antimicrobial and antioxidant activities of 2-[1-{3, 5-diaryl-4, 5-dihydro-1 H-pyrazolenyl}]4-(4-nitrophenyl)-[1, 3]-thiazoles. *Medicinal Chemistry Research*, 2013. 22(4): p. 1689-1699.
  19. Mushtaque, M., et al., Experimental and theoretical studies of a pyrazole-thiazolidin-2, 4-di-one hybrid. *Journal of Molecular Structure*, 2017. 1141: p. 417-427.
  20. Karim, H.A., A.M. Raauf, and K.F. Ali, Synthesis and preliminary pharmacological evaluation of some new triazole derivatives bearing nabumetone moiety targeting cyclooxygenase enzyme. *Systematic Reviews in Pharmacy*, 2021. 12(1): p. 190-195.
  21. Asiri, A.M., et al., Green synthesis, characterization, photophysical and electrochemical properties of bis-chalcones. *Int. J. Electrochem. Sci*, 2014. 9: p. 799-809.
  22. Daina, A., O. Michielin, and V. Zoete, SwissADME: a free web tool to evaluate pharmacokinetics, drug-likeness and medicinal chemistry friendliness of small molecules. *Scientific reports*, 2017. 7(1): p. 1-13.
  23. Nawaz, F., et al., 3'- (4- (Benzyloxy) phenyl)-1'- phenyl- 5- (heteroaryl/aryl)- 3, 4- dihydro-1' H, 2H- [3, 4'- bipyrazole]- 2- carboxamides as EGFR kinase inhibitors: Synthesis, anticancer evaluation, and molecular docking studies. *Archiv der Pharmazie*, 2020. 353(4): p. 1900262.
  24. Park, J.H., et al., Erlotinib binds both inactive and active conformations of the EGFR tyrosine kinase domain. *Biochemical Journal*, 2012. 448(Pt 3): p. 417.
  25. Mohammed, A.W., I.S. Arif, and G.A. Jasim, The Cytotoxic Effect of Metformin on RD Cell Line. *Al-Mustansiriyah Journal of Pharmaceutical Sciences (AJPS)*, 2019. 19(1): p. 85-94.
  26. Rodgers, E.H. and M.H. Grant, The effect of the flavonoids, quercetin, myricetin and epicatechin on the growth and enzyme activities of MCF7 human breast cancer cells. *Chemico-biological interactions*, 1998. 116(3): p. 213-228.
  27. Vijayarathna, S. and S. Sasidharan, Cytotoxicity of methanol extracts of *Elaeis guineensis* on MCF-7 and Vero cell lines. *Asian pacific journal of tropical biomedicine*, 2012. 2(10): p. 826-829.
  28. Sebaugh, J., Guidelines for accurate EC50/IC50 estimation. *Pharmaceutical statistics*, 2011. 10(2): p. 128-134.
  29. Adnan, A.M.A., M.F. Mahdi, and A. kareem Khan, Design, Synthesis, and Acute Anti-inflammatory Assessment of New 2-methyl Benzimidazole Derivatives Having 4-Thiazolidinone Nucleus. *Al-Mustansiriyah Journal of Pharmaceutical Sciences (AJPS)*, 2019. 19(4): p. 151-160.
  30. Pajouhesh, H. and G.R. Lenz, Medicinal chemical properties of successful central nervous system drugs. *NeuroRx*, 2005. 2(4): p. 541-553.
  31. Verdonk, M.L., et al., Improved protein–ligand docking using GOLD. *Proteins: Structure, Function, and Bioinformatics*, 2003. 52(4): p. 609-623.
  32. Adeniyi, A.A. and P.A. Ajibade, Comparing the suitability of autodock, gold and glide for the docking and predicting the possible targets of Ru (II)-based complexes as anticancer agents. *Molecules*, 2013. 18(4): p. 3760-3778.
  33. Alvarez, J. and B. Shoichet, Virtual screening in drug discovery. 2005: CRC press.
  34. Downs, R.P., et al., Design and development of FGF-23 antagonists: Definition of the pharmacophore and initial structure-activity relationships probed by synthetic analogues. *Bioorganic & medicinal chemistry*, 2021. 29: p. 115877.
  35. Panicker, N.G., et al., Organic extracts from *Cleome droserifolia* exhibit effective caspase-dependent anticancer activity. *BMC complementary medicine and therapies*, 2020. 20(1): p. 1-13.

## الارساء الجزيني و تحضير ودراسات ADME لمشتقات بيرازولين جديدة كعوامل محتملة مضادة للسرطان

عمار ك. وبدان<sup>1,2</sup>, منذر ف. مهدي<sup>2</sup>, اباد ك. خان<sup>2</sup>

<sup>1</sup>دائرة صحة المثلى , وزارة الصحة ,العراق

<sup>2</sup>كلية الصيدلة , الجامعة المستنصرية , بغداد ,العراق

يعتبر مرض السرطان من أهم قضايا الصحة العامة في جميع أنحاء العالم. ولا تزال الآثار الجانبية الضارة للعلاجات الكيميائية المضادة للسرطان تهدد جودة حياة المرضى. ولكشف انواع جديدة من الادوية المضادة للسرطان ، تم تصنيع سلسلة من مشتقات البيرازولين وتقييمها كأدوية مضادة للسرطان. تم تصنيع المشتقات الجديدة من خلال دمج جزئ البيرازولين الدوائي في جزيئة النابوميتون كجزيء ابتدائي ومشتقات الجالكون كنواتج وسطية . تم تخليق هذه المشتقات الجديدة بنجاح بكميات جيدة وتأكيد التركيب الكيميائي عن طريق التحاليل الطيفية <sup>1</sup>H-NMR و FT-IR. اجريت دراسة فحص الارساء الجزيني للمركبات عن طريق برنامج GOLD suite بالمقارنة مع دواء Erlotinib المعروف كمثبط لأنزيم Tyrosine kinase واطهرت المركبات نتائج عالية جدا وكانت هذه النتائج متوافقة الى حد ما مع النتائج التجريبية النهائية. تم تقييم الفعالية المضادة للسرطان للمركبات النهائية المصنعة على خلايا سرطان الرئة (A549), المركبات (P1,P2,P3,P4) أظهرت نتائج متوسطة الى عالية وكانت قيم IC<sub>50</sub> هي (15,409 , 7,24 , 27,05 , 22,45 مايكرومولار) على التوالي مقارنة مع دواء Erlotinib الذي اعطى فعالية مع قيمة IC<sub>50</sub> (25.23 مايكرومولار). بينما المركبين P6 و P7 اعطى نتائج ضعيفة. كذلك تم قياس الخصائص الحركية الدوائية والفيزيائية الكيميائية للمركبات المصنعة باستخدام SwissADME server واطهرت النتائج ان جميع المركبات المصنعة لديها توافر حيوي فموي وامتصاص عالي من القناة الهضمية.